

# 1 Neuronal components of evaluating the human origin of abstract shapes

2 Hagar Goldberg<sup>1</sup>, Yuval Hart<sup>2</sup>, Avraham E Mayo<sup>3,4</sup>, Uri Alon<sup>3,4</sup> and Rafael Malach<sup>1</sup>

3 • Department of Neurobiology, Weizmann Institute of Science, Rehovot, Israel

4 • School of Engineering and Applied Sciences, Harvard University, Cambridge, MA USA

5 • Department of Molecular Cell Biology, Weizmann Institute of Science, Rehovot, Israel

6 • The Theatre Lab, Weizmann Institute of Science, Rehovot, Israel

7 Corresponding author. Fax: +972 8 9344131. E-mail addresses: rafi.malach@weizmann.ac.il, rafi.malach@gmail.com (R. Malach).

8

## 9 Abstract

10 Communication through visual symbols is a key aspect of human culture. However, to what  
11 extent can people distinguish between human-origin and artificial symbols, and the neuronal  
12 mechanisms underlying this process are not clear. Using fMRI we contrasted brain activity  
13 during presentation of human-created abstract shapes and random-algorithm created shapes,  
14 both sharing similar low level features.

15 We found that participants correctly identified most shapes as *human* or *random*. The lateral  
16 occipital complex (LOC) was the main brain region showing preference to human-made shapes,  
17 independently of task. Furthermore, LOC activity was parametrically correlated to beauty and  
18 familiarity scores of the shapes (rated following the scan). Finally, a model classifier based only  
19 on LOC activity showed human level accuracy at discriminating between human-made and  
20 randomly-made shapes.

21 Our results highlight the sensitivity of the human brain to social and cultural cues, and point to  
22 high-order object areas as central nodes underlying this capacity.

23

## 24 Introduction:

25 Humans are social and tuned to social cues. They therefore need to distinguish true social cues  
26 from other stimuli. Previous studies have shown that human observers can distinguish biological  
27 motion from random motion, even in impoverished stimuli such as point-light displays  
28 (Johansson, 1973). This is suggested to be an intrinsic ability of the visual system, which has  
29 evolved to preferentially attend to other humans, as shown in newborn babies (Simion et al.,  
30 2008). These findings suggest that essential information such as social recognition can be  
31 derived from minimalistic dynamic displays. In addition to direct communication (through verbal  
32 and body language) human culture has ways of indirect communication through visual symbols -

33 a conventional representation of concepts through scripts and art; starting from cave paintings  
34 (Chauvet et al., 1996), and continuing nowadays with symbols such as emoticons.  
35 Similarly to the way humans can distinguish human walk from random motion generated by spot  
36 light displays, we hypothesize that humans can successfully recognize abstract shapes that have  
37 been generated by other humans compared to similar shapes created randomly. We further  
38 hypothesize that the neuronal mechanisms that underlie this capacity are likely to be ingrained in  
39 core systems and hence independent of the task performed.  
40 What could be the aspects of the shapes that underlie the ability of participants to categorize  
41 them into *human* vs. *random*? The symbolic meaning of a shape and its familiarity can serve to  
42 assess the shape's origin. Another relevant feature is the shape's aesthetic value, if indeed people  
43 tend to create more beautiful shapes. Thus, in the present study we focused on beauty and  
44 familiarity- i.e. iconicity - the sense that a shape represents a familiar icon. We also examined the  
45 inverse of familiarity- i.e. "weirdness"- a subjective sense that a figure is strange and unfamiliar.  
46 Both beauty and weirdness are intuitive and powerful yet subjective impressions which are  
47 difficult to define. Substantial work has suggested beauty and weirdness carry evolutionary  
48 advantages. For example, neuro-imaging study showed overlap in brain regions which function  
49 both during processing of aesthetic artworks and during appraisal of evolutionary important  
50 objects (e.g. attractive potential mates, or desirable food) (Brown et al., 2011). Visual artistic  
51 representations of beauty (Kawabata and Zeki, 2004, Di Dio et al., 2007, Ishizu and Zeki, 2011,  
52 Cattaneo et al., 2015, Vartanian and Goel, 2004, Lacey et al., 2011) or naturalistic stimuli  
53 beyond the arts domain (Brown et al., 2011, Chatterjee et al., 2009, Kirk, 2008, Lacey et al.,  
54 2011) were showed to be linked to experience of reward, pleasure, and attitudes to external  
55 information (approach/withdrawal). Similarly, the concept of weirdness was attributed to signals  
56 of danger and risk (Rotshtein et al., 2001). Sensing beauty and weirdness thus seem important for  
57 human behavior and survival, but we have little understanding of their neuronal correlates.  
58 Another line of work considered the contrast between artificial and familiar images in a number  
59 of studies of the human visual cortex (e.g. Fourier descriptors, and scrambled images; Lerner et  
60 al., 2002, Tsao et al., 2003, Aalto et al., 2002, Murray et al., 2002, Malach et al., 1995). Visual  
61 objects such as face images were rendered bizarre by inverting internal face features (Rotshtein  
62 et al., 2001). These studies showed an increased activity of high order object areas (lateral  
63 occipital complex - LOC) to coherent objects whether they are familiar or unfamiliar (Malach et

64 al., 1995, Kanwisher et al., 1997, Kanwisher et al., 1996, Grill-Spector et al., 2001, Rotshtein et  
65 al., 2001).

66 However, in previous work a control over low-level features was lacking. In fact, we are not  
67 aware of systematic study that directly compared brain activation to human-generated vs.  
68 randomly generated shapes constructed of similar low-level components. Furthermore the  
69 contribution of beauty and familiarity to the ability to evaluate human origin of shapes has not  
70 been explored directly in previous research.

71 To address these issues, we examined, using fMRI, human perception of simple shapes made by  
72 other humans, compared to similar shapes generated by an artificial algorithm. We specifically  
73 examined to what extent brain regions respond differentially to these two categories - and to  
74 what extent the beauty, iconicity and weirdness dimensions contribute to this differentiation.  
75 To this end we employed a novel design in which a large group of 101 people were asked to  
76 create simple shapes and to rank them according to how appealing they were (interesting and  
77 beautiful) (Noy et al., 2012). Additional shapes were generated by an artificial, random walk  
78 algorithm sampling from the space of all possible shapes and excluding shapes that were  
79 generated by human observers. The generated shape ensemble included a wide spectrum of  
80 beauty and familiarity levels.

81 We found that participants which were unfamiliar with the shapes were able to successfully  
82 distinguish between human and random origin shapes. Our brain imaging results show that LOC  
83 activity was significantly higher for the human-made shapes compared to the *random* ones.  
84 Furthermore, this differential activity was a combined result of a positive correlation to beauty  
85 and iconicity (familiarity) and a negative correlation to weirdness (unfamiliarity) of the abstract  
86 shapes regardless of task. Our results point to the high-order object related complex (LOC -  
87 Malach et al., 1995) as a pivotal node in endowing human observers with the ability to recognize  
88 shared symbolic meaning and distinguish human from artificially created shapes.

## 89 **Results:**

90 Here we aimed to study the behavioral and neuronal mechanisms of distinguishing whether an  
91 abstract shape was created by a human from a given space of shapes or by an algorithm that  
92 makes a random choice from the same space of shapes. We used a rich yet fully determined  
93 space of shapes, made of ten contiguous squares. Shapes were built by either 101 human players  
94 in a computer-shape-generation game (see methods and Noy et al., 2012) or a random choice

95 algorithm from the same space of shapes. Thus, we contrasted algorithm-created with human-  
96 created abstract shapes having similar low-level features. The human-created shapes were further  
97 subdivided into three groups of different appeal ratings (by their human creators, see Methods).  
98 Subjects unfamiliar with the shapes underwent fMRI scanning while watching the shapes in a  
99 block design. The shapes were presented in two different experiments. In the first, subjects  
100 performed a color discrimination task (experiment and task 1), and in the second, a human vs.  
101 random algorithm origin discrimination task (experiment and task 2). Following the scan,  
102 subjects gave their subjective evaluations of beauty, weirdness and iconicity of the shapes (see  
103 Methods for details).

104  
105 Behavioral results: Subjects successfully distinguished between most human and random  
106 creation shapes (Fig. 2a). Most categories were successfully classified by the subjects (85-90%  
107 accuracy), except *not chosen* category which was correctly classified (as *human*) in only 30% of  
108 the cases (chance level = 50%). This difference in success rate between *not chosen* category and  
109 the other categories was significantly lower (Mann-Whitney  $U = 0$ ,  $n_1 = n_2 = 7$   $p < 0.005$ , two-  
110 tailed). The difference between all other categories was not significant. A bias-free signal  
111 detection analysis indicated that subjects were able to reliably distinguish between human and  
112 random made shapes ( $N = 13$ , mean  $d' = 2.03$ ,  $SE = \pm 0.34$ ). No difference in reaction times was  
113 found between the four categories in both experiments.  
114 Three subjective aspects of the shapes were examined; beauty, weirdness and iconicity.  
115 Weirdness and iconicity scores complemented each other – while weirdness focused mainly on  
116 the level of unfamiliarity of a shape, iconicity reflected the level of familiarity and distinct  
117 meaning. The classification to human origin was best modeled by the interaction of the beauty  
118 and weirdness scores rather than the two scores separated  
119 ( $P(\text{human}) = (1 + 13.7 e^{-6.6 WB})^{-1}$ ) (see Methods and SI). Beauty scores were lowest for  
120 *random* and *not chosen* shapes, and were significantly higher for *chosen* and even higher for *top*  
121 *rate* (Mann-Whitney between *random* and *not chosen*:  $U = 20$ ,  $n_1 = n_2 = 7$ ,  $p = 0.521$ , two-tailed;  
122 between all other categories:  $U = 0$ ,  $n_1 = n_2 = 7$ ,  $p < 0.005$ , two-tailed. see Fig. 2b). Thus  
123 indicating cross population consistency between the creators of the shapes and the scanned  
124 participants.

125 Weirdness scores on the other hand distinguished between *human* and *random* categories; the  
126 *random* category received the highest score, *not chosen* received a significantly lower score,  
127 *chosen* and *top rated* received the lowest scores, significantly different from the first two (Mann-  
128 Whitney between *chosen* and *top rated*:  $U = 0.531$ ,  $n_1 = n_2 = 7$ ,  $p = 0.08$ , two-tailed; between all  
129 other categories:  $U = 1$ ,  $n_1 = n_2 = 7$ ,  $p < 0.005$ , two-tailed. see Fig. 2c). Thus, subjective beauty  
130 was positively correlated, and weirdness was negatively correlated to classification as *human*.  
131 Furthermore each parameter separated between different shape categories.

132  
133 Brain imaging results: In order to examine a possible implicit differentiation between human-  
134 made shapes and randomly made shapes, a direct contrast of BOLD activity (task 1) between  
135 *human* blocks and *random* blocks was conducted. The contrast map (Fig. 3) revealed highly  
136 localized preferential activations to *human* vs. *random* in the lateral occipital complex (LOC,  
137 Malach et al., 1995). Preferential activation to *random* shapes was spread over a wider range of  
138 the cortex, particularly in parietal and frontal regions. Its most significant activation was located  
139 in the inferior parietal gyrus (IFG).

140 Cross-task ROI analysis demonstrated a consistently stronger response to *human* blocks relative  
141 to *random* blocks in bilateral LOC in both tasks (paired t test; (experiment 1) left LOC,  $N = 17$ ,  $t$   
142  $= 2.74$ ,  $p < 0.05$ ; right LOC,  $N = 17$ ,  $t = 3.92$ ,  $p < 0.005$ ; (experiment 2) left LOC,  $N = 15$ ,  $t =$   
143  $3.93$ ,  $p < 0.005$ ; right LOC,  $N = 15$ ,  $t = 3.29$ ,  $p < 0.05$ ). ROI analysis inspecting the averaged  
144 LOC activity (beta weight) per category revealed a gradual positive response in bilateral LOC  
145 along the "appeal" axis (Fig 3c). *Random* shapes showed the lowest response in LOC, top rated  
146 showed the highest response (followed by not chosen and chosen respectively) (One way  
147 repeated measures ANOVA; (experiment 1) left LOC,  $N = 17$ ,  $F = 2.751$  not significant, Linear  
148 trend:  $F = 5.174$ ,  $p < 0.05$ ; right LOC,  $N = 17$ ,  $F = 4.35$ ,  $p < 0.05$ , Linear trend:  $F = 7.974$ ,  $p <$   
149  $0.05$ ; (experiment 2) left LOC,  $N = 15$ ,  $F = 6.145$ ,  $p < 0.05$ , Linear trend:  $F = 28.721$ ,  $p < 0.0005$ ;  
150 right LOC,  $N = 15$ ,  $F = 8.052$ ,  $p < 0.0005$ , Linear trend:  $F = 26.281$ ,  $p < 0.0005$ ).

151 Since beauty, weirdness and iconicity scores were predictive for blocks classification  
152 (*human/random*) we wanted to study their neuronal correlates. A whole brain parametric GLM  
153 analysis was therefore conducted (Fig. 4). The results revealed a consistent parametric  
154 relationship between LOC activity to beauty, weirdness and iconicity measures regardless of task  
155 (color/ shape origin discrimination). Parametric brain maps for beauty scores show focused

156 activation in the LOC. However in frontal areas, weirdness and iconicity showed a task-related  
157 selectivity: in task 1 frontal region such as dorsal premotor cortex and inferior frontal gyrus  
158 (IFG) were parametrically correlated to weirdness (positive) and iconicity (negative). In task 2  
159 lateral frontal cortex and superior parietal lobe showed parametric correlation to both weirdness  
160 (negative) and iconicity (positive) measures (Fig. 4). Finding a common neuronal network to  
161 both weirdness and iconicity with inverse correlation, supports the idea that these parameters  
162 reflect two opposite aspects of shapes familiarity and symbolic meaning.

163 In order to disentangle the coupling between the subjective parameter of beauty and the objective  
164 parameter of symmetry (Spearman correlation,  $r = 0.92$ ,  $p < 5 * 10^{-11}$ ), we calculated a subjective  
165 beauty score – blocks were ranked by their beauty score per subject, and then beauty scores of  
166 blocks with same ranking were averaged across subjects. The result is a perceptual beauty score  
167 which is independent of physical attributes such as symmetry. ROI analysis demonstrated a  
168 significant positive correlation between both symmetry/beauty and LOC activity (averaged  
169 normalized beta weights). However, the subjective beauty scores showed a significantly higher  
170 correlation compared to the symmetry scores (Spearman correlation; (experiment 1) left LOC,  
171 Symmetry:  $r = 0.4$ , ns; Beauty:  $r = 0.5$ ,  $p < 0.005$ ; right LOC, Symmetry:  $r = 0.47$ ,  $p < 0.05$ ;  
172 Beauty:  $r = 0.72$ ,  $p < 5 * 10^{-5}$ ; (experiment 2) left LOC, Symmetry:  $r = 0.57$ ,  $p < 0.005$ ; Beauty:  $r$   
173  $= 0.69$ ,  $p < 5 * 10^{-5}$ ; right LOC, Symmetry:  $r = 0.5$ ,  $p < 0.05$ ; Beauty:  $r = 0.81$ ,  $p < 5 * 10^{-7}$ , see Fig.  
174 5). The correlation scores were further compared using bootstrapping method, where data points  
175 were randomly chosen (with replacements) from each dataset and the correlation was calculated.  
176 Each process was repeated 1000 times. (Spearman correlation; (experiment 1) left LOC,  
177 Symmetry:  $r = 0.28 \pm 0.17$ , Beauty:  $r = 0.54 \pm 0.13$ ,  $d' = 1.2$ ; right LOC, Symmetry:  $r = 0.18 \pm 0.17$ ,  
178 Beauty:  $r = 0.72 \pm 0.18$ ,  $d' = 2.9$ ; (experiment 2) left LOC, Symmetry:  $r = 0.35 \pm 0.15$ , Beauty:  $r =$   
179  $0.69 \pm 0.06$ ,  $d' = 2.1$ ; right LOC, Symmetry:  $r = 0.28 \pm 0.16$ , Beauty:  $r = 0.81 \pm 0.05$ ,  $d' = 3.1$ . All  
180 values are Mean  $\pm$ STD,  $N_{(\text{symmetry})} = 16$ ,  $N_{(\text{beauty})} = 13$ ). According to these results perceptual  
181 beauty showed a graded response across the entire dynamic range enhancing correlation and  
182 significance while symmetry correlation highly depended on the points chosen as evident from  
183 its large correlation variation (Fig. 5).

184 Iconicity group scores were also correlated to LOC activity; Spearman correlation; (experiment  
185 1) left LOC,  $r = 0.51$ ,  $p < 0.01$ ; right LOC,  $r = 0.65$ ,  $p < 0.0005$ . (experiment 2) left LOC,  $r =$   
186  $0.65$ ,  $p < 0.0005$ ; right LOC,  $r = 0.57$ ,  $p < 0.005$ .

187 Lastly, we tested whether one could infer a shape's origin by the beta activity of LOC. We  
188 compared the average LOC activity for each block with its probability to be classified as human.  
189 We fitted a non-linear hyperbolic tangent classifier with a random partial sample of data points  
190 (23/28) and iterated the process 1000 times. We found that the averaged fitted function predicted  
191 78% of the shapes accurately by using the average beta activity of the block (compared to 50%  
192 for chance performance). Interestingly, the classifier's ability resembled the subject's behavioral  
193 results with 86% correct in *random*, *chosen* and *top-rated* categories, and only 57% in the *not-*  
194 *chosen* category. Thus, LOC activity might serve as a predictor to the shape's origin.

195

### 196 **Discussion:**

197 The human brain is skilled in distinguishing between the familiar and the strange, between the  
198 natural and the artificial, and here we examined its ability to distinguish between human and  
199 random creations. We showed here a tight connection between behavior and brain function  
200 related to the process of identifying the origin of human-generated versus random abstract  
201 shapes. Our findings revealed that human subjects could correctly identify shapes as human  
202 made or randomly made. Subjects showed a general agreement that *random* shapes appeared  
203 weirder. Moreover their aesthetic evaluation of the shapes (Fig. 2b) was very similar to the  
204 evaluation made by the shapes' creators (the three categories of human made shapes - see  
205 methods). These findings suggest a general agreement among individuals about what is  
206 considered human, meaningful and beautiful.

207 While previous studies used complex naturalistic images or objects, in the current study we used  
208 relatively simple and well-controlled shapes. Although similar in low level features, some of  
209 them (*random* shapes) were out of the common human scheme as manifested by the players  
210 playing the game. Indeed they were never created by human players (although probabilistically  
211 they should have been created), and they were perceived differently by the human brain.

212 Brain activity - specifically, the LOC, showed preferential activation to *human* relative to  
213 *random* blocks even in task 1 (color discrimination) in which attention was targeted to color  
214 rather than shapes. This supports our hypothesis that the human brain is capable of recognizing  
215 human creation even when not explicitly instructed to do so.

216 The LOC, well established as a hub of visual object recognition (Malach et al., 1995, Grill-  
217 Spector et al., 2001) - was the central region showing a preferred activation to human-made

218 shapes compared to *random* shapes (task independent). The complementary, preferred activation  
219 to *random* shapes was found in parietal regions, motor cortex and most significantly in the  
220 inferior frontal gyrus (IFG, see figure 3). These findings are compatible with previous studies  
221 which reported that IFG is responsive to unexpected stimuli (Huettel and McCarthy, 2004), and  
222 to incongruent stimuli specifically within a social context (Shibata et al., 2011).

223 We examined 3 subjective shape characteristics with predictive value to classify as  
224 *human/random*; beauty, weirdness and iconicity. Using a whole brain analysis exploratory  
225 approach - we searched brain networks which were parametrically connected to each external  
226 measure. These analyses (Fig. 4) showed that LOC was a central node - parametrically correlated  
227 to shapes' beauty, weirdness (inversely correlated) and iconicity. Moreover, using LOC activity  
228 might allow predicting shape's origin with human level accuracy (Fig. 6). Thus, our findings  
229 point to the LOC as a central node for human vs. random origin, with shape's beauty and  
230 symbolic meaning playing a role in that evaluation.

231  
232 **Brain and beauty:**  
233 Previous studies of beauty, focusing on response to visual arts or objects perception, found  
234 activations in reward related areas, such as the orbito-frontal cortex (Kawabata and Zeki, 2004,  
235 Brown et al., 2011, Ishizu and Zeki, 2011, Kirk, 2008, Lacey et al., 2011, Cela-Conde et al.,  
236 2004), in emotion related areas like the amygdala (Brown et al., 2011, Di Dio et al., 2007, Ishizu  
237 and Zeki, 2011) and insula (Brown et al., 2011, Di Dio et al., 2007) and also in motor areas  
238 (Kawabata and Zeki, 2004, Ishizu and Zeki, 2011), pointing to a link between the experience of  
239 beauty to reward or information gathering and response upon it.

240 Recent studies also point to high order visual areas, and specifically the LOC, as an aesthetic  
241 center in the brain (Cattaneo et al., 2015, Chatterjee et al., 2009, Kirk, 2008, Lacey et al., 2011,  
242 Vartanian and Goel, 2004). Some reported that high order visual areas show preferential activity  
243 for aesthetic value only for representational art and not for abstract art (Cattaneo et al., 2015,  
244 Vartanian and Goel, 2004).

245 In the current study we explored which brain regions were sensitive to the beauty of abstract  
246 shapes. Our results revealed a consistent (experiments 1 and 2) positive parametric correlation  
247 between subjective beauty scores and bilateral LOC (Fig. 4a). The consistency and specificity of

248 LOC in beauty analyses, suggests that beauty evaluation of abstract shapes is an automatic -  
249 bottom up process which is less dependent on the attention to the shape.

250 Previous studies pointed to the LOC as a central player in symmetry evaluation (Hodgson, 2009,  
251 Chatterjee et al., 2009, Beck et al., 2005, Sasaki et al., 2005). In the present study symmetry  
252 indeed showed a significant correlation to beauty ratings. Importantly, the correlation between  
253 LOC activity and symmetry was significantly weaker and less reliable compared to the beauty  
254 score correlations (Fig. 5). Thus, our paradigm of abstract shapes allowed the decoupling of the  
255 symmetry measure from that of the beauty scores. Our results show that subjective beauty  
256 evaluation is better correlated to LOC activity compared to shapes' symmetry.

257

258 Brain and familiarity:

259 According to our results - both weirdness and iconicity, measures of familiarity and symbolic  
260 meaning, were correlated with LOC activation. Previous works showed increased activation in  
261 LOC which was similar for familiar and unfamiliar objects as long as the object is a coherent one  
262 (Malach et al., 1995, Kanwisher et al., 1997, Kanwisher et al., 1996, Grill-Spector et al., 2001),  
263 tracing a difference in activation between coherent objects response to non-coherent ones (using  
264 Fourier descriptors, and scrambled images; Lerner et al., 2002, Tsao et al., 2003, Aalto et al.,  
265 2002, Murray et al., 2002, Malach et al., 1995). This is compatible with the earlier finding of an  
266 enhanced activity in mid-fusiform gyrus in a response to abstract shapes, associated with long-  
267 term familiarization (Gauthier et al., 1999). Similarly, right LOC showed enhanced activity to  
268 abstract object structures following a short-term learning (familiarization) (de Beeck et al.,  
269 2006). Furthermore, LOC preferential activity to familiar (iconic) objects was shown in a visual  
270 imagery with haptic perception task (Deshpande et al., 2010, Lacey et al., 2010).

271 Our abstract shapes paradigm introduced a broad range of familiarity levels, which allowed to  
272 explore the effect of familiarity on LOC activity on a graded scale instead of a binary approach  
273 (familiar/unfamiliar) and without distortion of object's features (Lerner et al., 2002, Tsao et al.,  
274 2003, Aalto et al., 2002, Murray et al., 2002, Malach et al., 1995, Rotshtein et al., 2001). Shapes  
275 with different familiarity levels manifested a difference in LOC activation although composed of  
276 similar low level features.

277 Interestingly, weirdness and iconicity showed inversed correlation patterns within very similar  
278 neuronal networks, supporting the idea that they reflect the two ends of shapes familiarity and

279 meaning (not only theoretically but also neuronal). While the beauty parametric analysis  
280 showed a consistent and local activity of LOC, both weirdness and iconicity parametric mapping  
281 showed a task dependent activation, and a broader network involvement, including frontal and  
282 parietal regions in addition to LOC (Fig. 4b,c).

283 It could have been argued that the identification of human origin shapes was mainly due to  
284 highly recognizable symbols (e.g. letters and digits). However- such iconic shapes were only a  
285 small portion (~10%) of the entire ensemble (sup Fig. 1). In fact, the shape ensemble introduced  
286 a gradient of iconicity as was shown by both ratings and brain responses. Furthermore, it has  
287 been well established that letters and digit representations are left- lateralized (Hasson et al.,  
288 2002, Fiez and Petersen, 1998, McCandliss et al., 2003) while we consistently found a slight  
289 right-hemisphere bias of the *human vs. random* contrast (sup Fig. 2).

290 De Beeck et al have showed an overall increased response to trained abstract objects compared  
291 to untrained abstract objects. Right LOC in particular showed the strongest increased response as  
292 a result to the training (de Beeck et al., 2006). In our study there was no formal training and all  
293 the shapes were novel, however we suggest that the human schema is an expression of an  
294 inherent training for social representations in the human mind. This schema led human players to  
295 explore certain shapes, and avoid other shapes (unlike the random walk algorithm), similarly this  
296 schema guided participants to successfully distinguish between human made and randomly made  
297 shapes. It is an open question whether this schema was developed as a result or is the source of  
298 human graphic communication. An interesting future avenue related to this question will be to  
299 investigate whether these findings are reproducible across cultures, within cultures, and in young  
300 infants. It will also be of interest to study whether humans on the autistic spectrum experience  
301 and neuronal process these shapes similarly to typical individuals.

302

303 Conclusion:

304 Our study examined the behavioral and neuronal components of evaluating human origin of  
305 abstract shapes. Our results point to high order object areas (LOC) as a central node in beauty  
306 representation, and in symbolic meaning attribution of abstract shapes. Both aspects had a  
307 significant contribution to the classification of shape origin as *human* or *random*, and may have a  
308 key role in visual human communication (such as visual art).

309

## 310 **Materials and methods:**

### 311 *participants:*

312 Seventeen healthy right handed subjects (ages  $28 \pm 3.8$ , 10 females) participated in the fMRI  
313 experiments. Fifteen of them participated in both experiments 1 and 2. Fourteen filled a beauty,  
314 iconicity and weirdness evaluation questionnaire post the fMRI scan.

315

### 316 *Task and stimuli:*

317 Shape stimuli. Shapes of ten contiguous identical green squares were created in a shape-search  
318 computer game, by either 101 human players or a random walk algorithm (Noy et al., 2012). In  
319 each shape, squares were connected by an edge. Players moved one square at a time to create  
320 new shapes. They were instructed to place beautiful and interesting shapes into a gallery by  
321 pressing a button. There was no limit to the gallery. Players played for 15 min and created about  
322 310 shapes, of which they chose 46 shapes on average to the gallery. At the end of the game,  
323 players chose the 5 most creative shapes from their own gallery. The shape space includes  
324 36,446 possible shapes.

325 Shapes were classified into four categories based on their origin (human/algorithm), and their  
326 appeal ratings (by their human creators). *Not chosen shapes* were created by human players but  
327 never chosen as beautiful shapes (by the players). *Chosen shapes* were created by human players,  
328 chosen as beautiful and interesting to the gallery but never rated as most creative shapes. *Top*  
329 *rated shapes* were created by human players, chosen as beautiful and interesting shapes and were  
330 rated by players as most creative shapes. *Random (Never human-created shapes)* were created  
331 only by a random walk algorithm (and never by human players) on the space of shapes, where  
332 the next shape is chosen randomly from neighboring shapes that are one move of a square away  
333 from the current shape. Length of walks was sampled from the distribution of walk lengths of the  
334 human players. For each category, the 20 most frequent shapes, i.e. the shapes that were the most  
335 common to many players (or random walks in the random category), were chosen for the fMRI  
336 experiment (see the shapes in sup. Fig. 1).

337

### 338 *Experimental design*

339 During the fMRI scan the created shapes were presented in homogeneous-category blocks lasting  
340 9 sec, followed by a 9 sec fixation screen. Each block consisted of 9 images (one second each);

341 eight images in light green and one image in dark green. Each category was presented in seven  
342 different blocks. To reduce scan novelty effect, an extra block (which was not analyzed) was  
343 added to the beginning of each experiment, 29 blocks were presented in total.

344 Each subject watched the same sequence of blocks twice (once for each task). In the first  
345 experiment (task 1) subjects were required to classify the stimuli according to color; light green  
346 (press 1) or dark green (press 2). In the second experiment (task 2) following each block,  
347 subjects were required to classify the shapes of the preceding block as human creation (press 1)  
348 or random algorithm creation (press 2).

349

### 350 *Subjective and objective shape evaluations*

351 Following the scan, subjects evaluated each shape's beauty level on a 1-4 scale (4 being most  
352 beautiful), chose the 20 weirdest shapes, and also chose the most iconic shapes in blocks of 20  
353 shapes.

354 Block's beauty score was calculated as the summation of beauty scores of all the shapes in the  
355 block. Weirdness and iconicity scores were calculated independently, in the same manner; A  
356 shape's weirdness/iconicity score was equal to the number of subjects which rate the shape as  
357 weird/iconic. A block's weirdness/iconicity score was calculated as the summation of  
358 weirdness/iconicity scores of all shapes in the block.  
359 In addition- the shapes were analyzed according to symmetry as an objective parameter. Block's  
360 symmetry was calculated as the summation of all rotation and reflection symmetry groups of all  
361 the shapes in the block.

362

### 363 *MRI Data Acquisition and Preprocessing*

364 The data were acquired on a 3 Tesla Trio Magnetom Siemens scanner at the Weizmann Institute  
365 of Science. Functional images of blood oxygenation level dependent (BOLD) contrast  
366 comprising of 46 axial slices were obtained with a T2\*-weighted gradient echo planar imaging  
367 (EPI) sequence ( $3 \times 3 \times 3$  mm voxel, TR = 3000 ms, TE = 30, flip angle =  $75^\circ$ , FOV 240 mm)  
368 covering the whole brain. Anatomical images for each subject were acquired in order to  
369 incorporate the functional data into the 3D Talairach space (Talairach and Tournoux, 1988) using  
370 3-D T1- weighted images with high resolution ( $1 \times 1 \times 1$  mm voxel, MPRAGE sequence, TR=  
371 2300 ms, TE= 2.98 ms).

372 The first 7 images of each functional scan (including the extra initial block and rest) were  
373 discarded. Functional scan preprocessing included 3D motion correction and filtering out of low  
374 frequency noise (slow drift), and spatial smoothing using an isotropic Gaussian kernel of 6 mm  
375 full-width-half-maximum (FWHM). The functional images were superimposed on 2D anatomic  
376 images and incorporated into the 3D data sets through trilinear interpolation. Statistical analysis  
377 was based on a general linear model in which all stimuli conditions were defined as predictors,  
378 and convolved with the hemodynamic response function (HRF).

379

#### 380 *Data analysis:*

381 In order to learn about the connection between shapes' characteristics, perception and brain  
382 activity several measurements were examined; Reaction times (both tasks), response accuracy  
383 (*human/random*, task2), subjective evaluations post-scan (beauty, weirdness and iconicity), and  
384 symmetry score.

385 To investigate a possible difference in reaction times between shape categories (*random, not*  
386 *chosen, chosen, top rated*), Mann-Whitney tests were calculated for experiment 1 and 2 within  
387 subject and between subjects. Aesthetic (beauty) ratings for each shape were collected by each  
388 subject post the scan (on a 1-4 scale). To control for difference in rating patterns each subject's  
389 ratings were Z normalized. Five GLM analyses were conducted; the first included four  
390 predictors: *random, not chosen, chosen, top rated*. A second GLM analysis with two predictors  
391 based on the category's creator: *human* or *random*. In addition, in order to relate subjective  
392 blocks' characteristics to brain activity, three parametric GLM analyses were conducted for  
393 beauty, weirdness and iconicity. In these multi-subject, random effect analyses each block of  
394 shapes received a weight according to its score (beauty/weirdness/iconicity) which was  
395 represented in the model as differential amplitude of the BOLD signal. Beauty, being an  
396 individual score calculated per subject separately, was z normalized between subjects.

397

398 Model selection of beauty and weirdness as well as beauty and iconicity fit to the probability to  
399 be classified as human was done based on the spearman correlation between model predictions  
400 and the Akaike information criterion (AIC). Models were generated as all possible combinations  
401 of the three parameters, either alone or coupled together. In order to have the monotonicity of the

402 two scores increase in the same direction, weirdness score was represented as  $e^{-Weirdness\ score}$   
403 (see SI for more details).

404  
405 In all GLM analyses beta coefficients were calculated for the regressors, and a Student's t-test  
406 was performed. Multi-subject analysis was based on a random-effect GLM. Multi-subject  
407 contrast maps (*human vs. random*, or *category vs. category*) were projected on an unfolded,  
408 inflated Talairach-normalized brain. Significance levels were calculated, taking into account the  
409 minimum cluster size and the probability threshold of a false detection of any given cluster. This  
410 was accomplished by a Monte Carlo simulation (cluster-level statistical threshold estimator in  
411 “Brain Voyager” software).

412 In the first experiment (task1) for *human vs. random* contrast (Fig. 3) a minimum cluster size of  
413 103 voxels was significant. A minimum cluster size of 71 voxels was significant for *top rated vs.*  
414 *chosen*, 78 voxels for both *top rated vs. not chosen*, and *chosen vs. not chosen* (sup Fig. 2a). The  
415 minimum significant cluster size for each *human category vs. random* (sup Fig. 2b) was 103  
416 voxels (*top rated*), 91 voxels (*chosen*) and 85 voxels (*not chosen*). For the parametric maps (Fig.  
417 4) a minimum cluster size of 84 voxels was significant for beauty in task 1, and 90 voxels in task  
418 2. For weirdness a minimum cluster size of 98 voxels was significant in task 1, and 105 voxels in  
419 task 2. For iconicity a minimum cluster size of 90 voxels was significant in task 1, and 104  
420 voxels in task 2.

#### 421 *ROI definition and analysis*

422 Analysis of LOC-relevant voxels was conducted by defining a group bilateral ROI within the  
423 LOC using the contrast *human > random* in one task, and sampled in the other task. Note that the  
424 inverted contrast i.e. *random > human* failed to reveal any voxels in the LOC region (see Fig. 3).  
425 The ROI's averaged beta weight (across voxels) was calculated per subject, for each predictor.  
426 Two-tailed paired t-tests (within subjects) were conducted between *human* and *random* beta  
427 weights for unaware (task 1) and aware (task 2) stimuli. A beta weight was extracted for each  
428 block and was plotted as a function of subjective beauty and symmetry (Fig. 5). Spearman  
429 correlation was calculated between participant's average beta for each block (averaged over each  
430 ROI) and their aforementioned features.

431

#### 432 **Acknowledgements**

433 We thank Nahum Stern, Fanny Atar and Dr. Edna Haran-Furman for their assistance in the imaging setup  
434 and fMRI data collection. We thank Dr. Lior Noy for developing the shapes-creation computer game.  
435 This study was supported by the EU FP7 VERE, EU HBP Flagship (R.M.), ICORE ISF grants (R.M.), the  
436 Helen and Martin Kimmel award (R.M.), the Braginsky Center for the Interface Between Science and  
437 Humanities (U.A). U.A. is the incumbent of the Abisch-Frenkel Professorial Chair.

438

## 439 **References**

440

441 AALTO, S., N T NEN, P., WALLIUS, E., METS HONKALA, L., STENMAN, H., NIEMI, P. &  
442 KARLSSON, H. 2002. Neuroanatomical substrata of amusement and sadness: a PET  
443 activation study using film stimuli. *Neuroreport*, 13, 67.

444 BECK, D. M., PINSK, M. A. & KASTNER, S. 2005. Symmetry perception in humans and  
445 macaques. *Trends in cognitive sciences*, 9, 405-406.

446 BROWN, S., GAO, X., TISDELLE, L., EICKHOFF, S. B. & LIOTTI, M. 2011. Naturalizing  
447 aesthetics: brain areas for aesthetic appraisal across sensory modalities. *Neuroimage*, 58,  
448 250-258.

449 CATTANEO, Z., LEGA, C., FERRARI, C., VECCHI, T., CELA-CONDE, C. J., SILVANTO, J.  
450 & NADAL, M. 2015. The role of the lateral occipital cortex in aesthetic appreciation of  
451 representational and abstract paintings: A TMS study. *Brain and cognition*, 95, 44-53.

452 CELA-CONDE, C. J., MARTY, G., MAESTÚ, F., ORTIZ, T., MUNAR, E., FERNÁNDEZ, A.,  
453 ROCA, M., ROSSELLÓ, J. & QUESNEY, F. 2004. Activation of the prefrontal cortex in  
454 the human visual aesthetic perception. *Proceedings of the National Academy of Sciences*  
455 *of the United States of America*, 101, 6321-6325.

456 CHATTERJEE, A., THOMAS, A., SMITH, S. E. & AGUIRRE, G. K. 2009. The neural  
457 response to facial attractiveness. *Neuropsychology*, 23, 135.

458 CHAUVET, J.-M., BRUNEL DESCHAMPS, E. & HILLAIRE, C. 1996. *Dawn of art: the*  
459 *Chauvet Cave: the oldest known paintings in the world*, HN Abrams.

460 DE BEECK, H. P. O., BAKER, C. I., DICARLO, J. J. & KANWISHER, N. G. 2006.  
461 Discrimination training alters object representations in human extrastriate cortex. *The*  
462 *Journal of Neuroscience*, 26, 13025-13036.

463 DESHPANDE, G., HU, X., LACEY, S., STILLA, R. & SATHIAN, K. 2010. Object familiarity  
464 modulates effective connectivity during haptic shape perception. *Neuroimage*, 49, 1991-  
465 2000.

466 DI DIO, C., MACALUSO, E. & RIZZOLATTI, G. 2007. The golden beauty: brain response to  
467 classical and renaissance sculptures. *PloS one*, 2, e1201.

468 FIEZ, J. A. & PETERSEN, S. E. 1998. Neuroimaging studies of word reading. *Proceedings of*  
469 *the National Academy of Sciences*, 95, 914-921.

470 GAUTHIER, I., TARR, M. J., ANDERSON, A. W., SKUDLARSKI, P. & GORE, J. C. 1999.  
471 Activation of the middle fusiform'face area'increases with expertise in recognizing novel  
472 objects. *Nature neuroscience*, 2, 568-573.

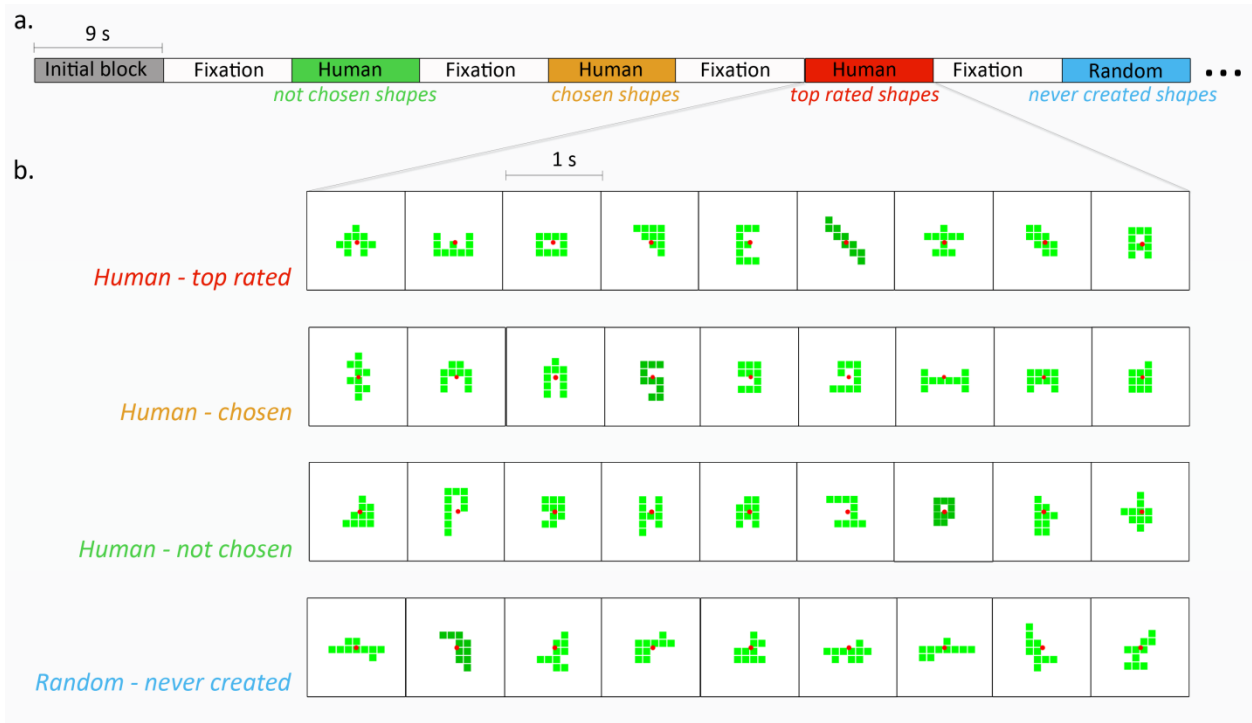
473 GRILL-SPECTOR, K., KOURTZI, Z. & KANWISHER, N. 2001. The lateral occipital complex  
474 and its role in object recognition. *Vision research*, 41, 1409-1422.

475 HASSON, U., LEVY, I., BEHRMANN, M., HENDLER, T. & MALACH, R. 2002. Eccentricity  
476 bias as an organizing principle for human high-order object areas. *Neuron*, 34, 479-490.

- 477 HODGSON, D. 2009. Evolution of the visual cortex and the emergence of symmetry in the  
478 Acheulean techno-complex. *Comptes Rendus Palevol*, 8, 93-97.
- 479 HUETTEL, S. A. & MCCARTHY, G. 2004. What is odd in the oddball task?: Prefrontal cortex  
480 is activated by dynamic changes in response strategy. *Neuropsychologia*, 42, 379-386.
- 481 ISHIZU, T. & ZEKI, S. 2011. Toward a brain-based theory of beauty. *PloS one*, 6, e21852.
- 482 JOHANSSON, G. 1973. Visual perception of biological motion and a model for its analysis.  
483 *Attention, Perception, & Psychophysics*, 14, 201-211.
- 484 KANWISHER, N., CHUN, M. M., MCDERMOTT, J. & LEDDEN, P. J. 1996. Functional  
485 imaging of human visual recognition. *Cognitive Brain Research*, 5, 55-67.
- 486 KANWISHER, N., WOODS, R. P., IACOBONI, M. & MAZZIOTTA, J. C. 1997. A locus in  
487 human extrastriate cortex for visual shape analysis. *Cognitive Neuroscience, Journal of*,  
488 9, 133-142.
- 489 KAWABATA, H. & ZEKI, S. 2004. Neural correlates of beauty. *Journal of Neurophysiology*,  
490 91, 1699-1705.
- 491 KIRK, U. 2008. The neural basis of object-context relationships on aesthetic judgment. *PloS one*,  
492 3, e3754.
- 493 LACEY, S., FLUECKIGER, P., STILLA, R., LAVA, M. & SATHIAN, K. 2010. Object  
494 familiarity modulates the relationship between visual object imagery and haptic shape  
495 perception. *Neuroimage*, 49, 1977-1990.
- 496 LACEY, S., HAGTVEDT, H., PATRICK, V. M., ANDERSON, A., STILLA, R.,  
497 DESHPANDE, G., HU, X., SATO, J. R., REDDY, S. & SATHIAN, K. 2011. Art for  
498 reward's sake: Visual art recruits the ventral striatum. *Neuroimage*, 55, 420-433.
- 499 LERNER, Y., HENDLER, T. & MALACH, R. 2002. Object-completion effects in the human  
500 lateral occipital complex. *Cerebral Cortex*, 12, 163-177.
- 501 MALACH, R., REPPAS, J., BENSON, R., KWONG, K., JIANG, H., KENNEDY, W.,  
502 LEDDEN, P., BRADY, T., ROSEN, B. & TOOTELL, R. 1995. Object-related activity  
503 revealed by functional magnetic resonance imaging in human occipital cortex.  
504 *Proceedings of the National Academy of Sciences*, 92, 8135-8139.
- 505 MCCANDLISS, B. D., COHEN, L. & DEHAENE, S. 2003. The visual word form area:  
506 expertise for reading in the fusiform gyrus. *Trends in cognitive sciences*, 7, 293-299.
- 507 MURRAY, S. O., KERSTEN, D., OLSHAUSEN, B. A., SCHRATER, P. & WOODS, D. L.  
508 2002. Shape perception reduces activity in human primary visual cortex. *Proceedings of*  
509 *the National Academy of Sciences*, 99, 15164-15169.
- 510 NOY, L., HART, Y., ANDREW, N., RAMOTE, O., MAYO, A. & ALON, U. Year. A  
511 quantitative study of creative leaps. In: Proc. Third Int. Conf. Comput. Creativity,  
512 Dublin, 2012. Citeseer, 72-76.
- 513 ROTSHTEIN, P., MALACH, R., HADAR, U., GRAIF, M. & HENDLER, T. 2001. Feeling or  
514 Features:: Different Sensitivity to Emotion in High-Order Visual Cortex and Amygdala.  
515 *Neuron*, 32, 747-757.
- 516 SASAKI, Y., VANDUFFEL, W., KNUTSEN, T., TYLER, C. & TOOTELL, R. 2005. Symmetry  
517 activates extrastriate visual cortex in human and nonhuman primates. *Proceedings of the*  
518 *National Academy of Sciences of the United States of America*, 102, 3159-3163.
- 519 SHIBATA, H., INUI, T. & OGAWA, K. 2011. Understanding interpersonal action coordination:  
520 an fMRI study. *Experimental Brain Research*, 211, 569-579.
- 521 SIMION, F., REGOLIN, L. & BULF, H. 2008. A predisposition for biological motion in the  
522 newborn baby. *Proceedings of the National Academy of Sciences*, 105, 809-813.

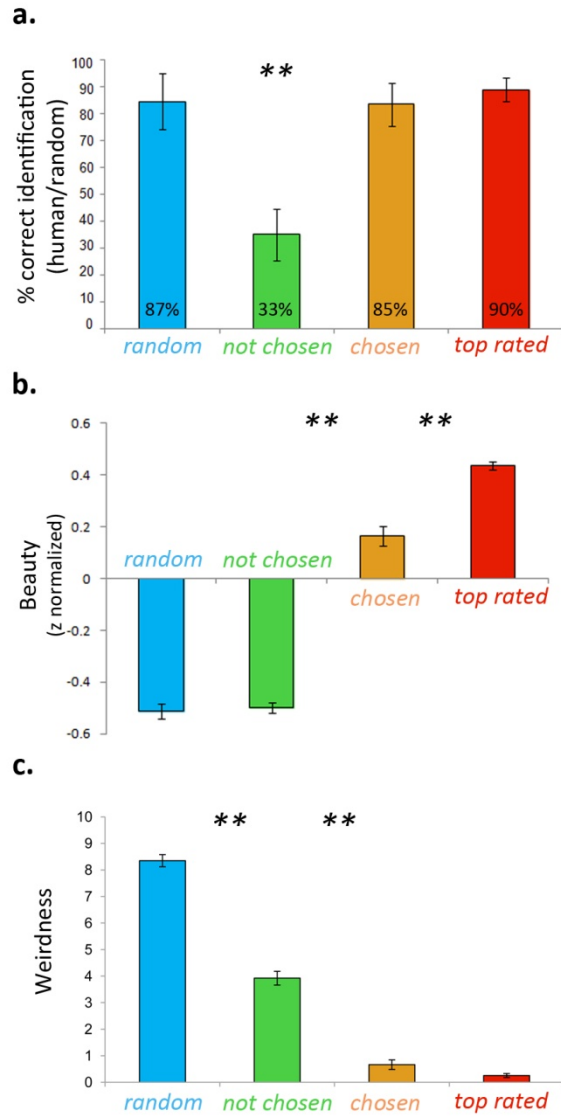
523 TALAIRACH, J. & TOURNOUX, P. 1988. Co-planar stereotaxic atlas of the human brain. 3-  
524 Dimensional proportional system: an approach to cerebral imaging.  
525 TSAO, D. Y., FREIWALD, W. A., KNUTSEN, T. A., MANDEVILLE, J. B. & TOOTELL, R.  
526 B. 2003. Faces and objects in macaque cerebral cortex. *Nature neuroscience*, 6, 989-995.  
527 VARTANIAN, O. & GOEL, V. 2004. Neuroanatomical correlates of aesthetic preference for  
528 paintings. *Neuroreport*, 15, 893-897.  
529  
530  
531  
532  
533  
534  
535  
536  
537  
538  
539  
540  
541  
542  
543  
544  
545  
546  
547  
548  
549  
550  
551  
552  
553  
554  
555  
556  
557  
558  
559  
560  
561  
562  
563  
564  
565  
566  
567

568



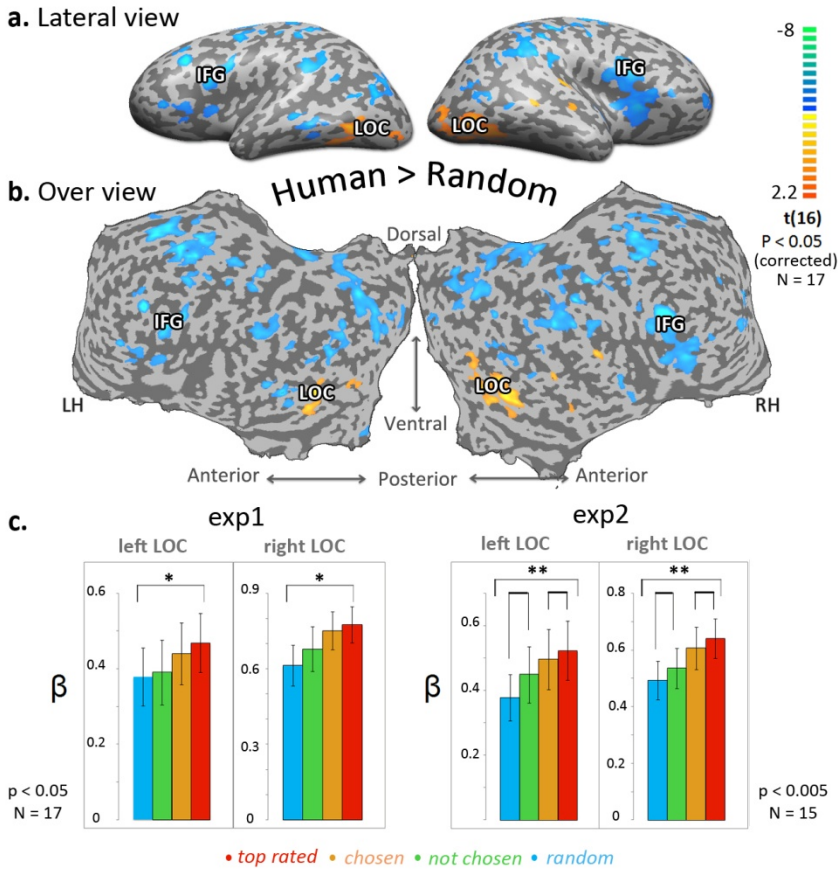
569  
570  
571  
572  
573  
574  
575  
576  
577

**Figure 1. Experimental design** .(a) Experimental protocol: shape images from four categories were presented in a block design with 9 second blocks, followed by 9 second fixation screen. Shape categorization was based on its creation process during a computer game in a previous work (Noy et al., 2012, see methods); *Top rated shapes* were created by human players and rated as most creative shapes. *Chosen shapes* were created by human players, chosen as beautiful shapes but never rated as most creative shapes. *Not chosen shapes* were created by human players but never chosen as beautiful shapes or rated (by the players). *Never created shapes* were created by a random algorithm, and never by human players. (b) Example for a block of each category. Each block included 9 images (one second each) of the same category; 8 images in light green and one in dark green.



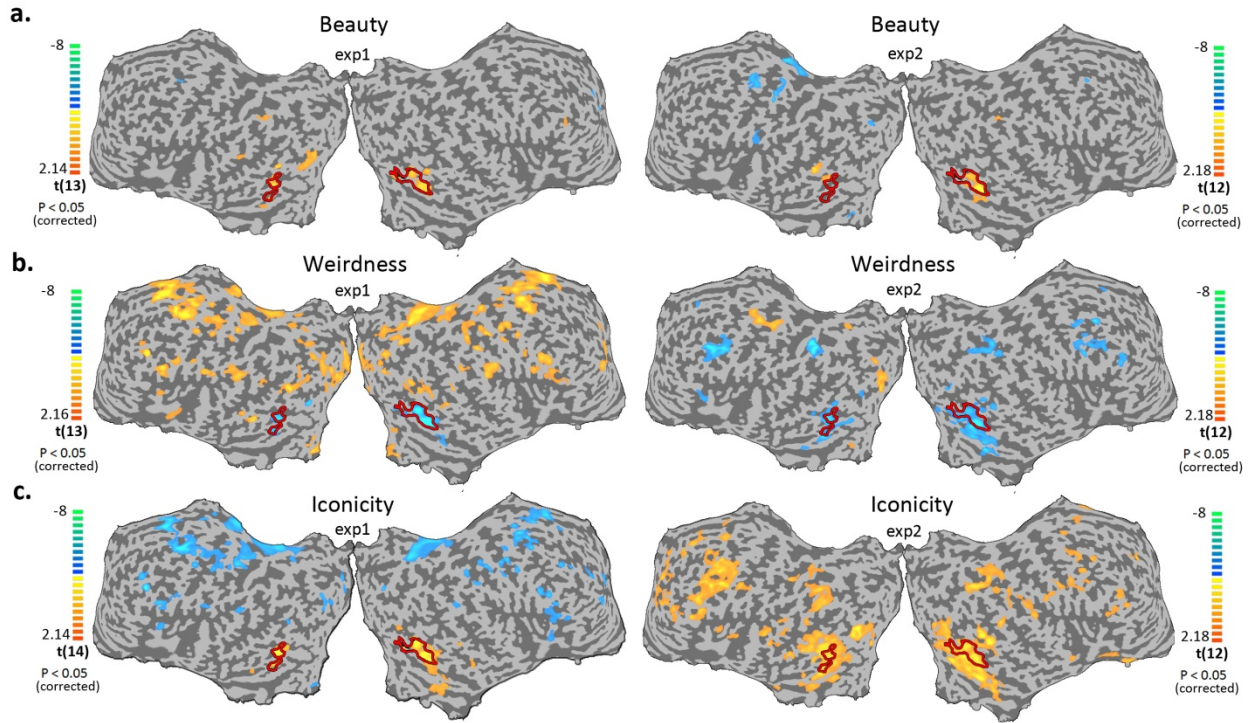
578  
579  
580  
581  
582  
583  
584  
585  
586  
587  
588  
589  
590  
591  
592  
593  
594  
595  
596  
597  
598  
599  
600  
601  
602

**Figure 2. Behavioral measurements** (a) Group's average percent success rate (human/random) in each category; *Human- top rated, Human- chosen, Human- not chosen, Algorithm-random*. Two-tailed, within subjects Mann-Whitney between categories,  $n_1 = n_2 = 7$ ,  $p < 0.005^{**}$ , error bars indicate the groups' standard error. (b) Group's average beauty scores per category (z-score normalized). (c) Group's average weirdness scores per category.



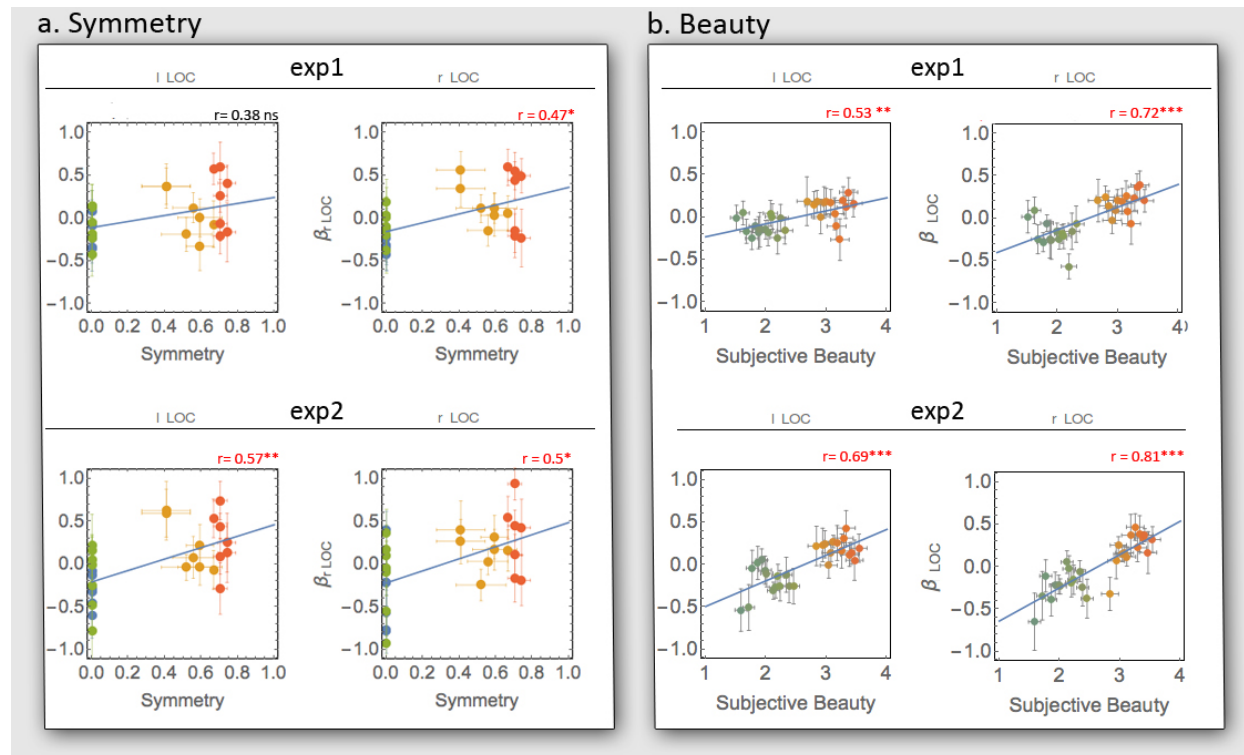
603  
604  
605  
606  
607  
608  
609  
610  
611  
612  
613  
614

**Figure 3. Comparison of Human and Random cortical activations.** All human generated shapes (*Human*) vs. computer generated shapes (*Random*) multi subjects activity map (experiment 1,  $N = 17$ , corrected  $p < 0.05$ ) is presented on an inflated cortex, in a lateral view (a) and unfolded cortex (b). Color scale indicates t values. Yellow-orange scale represents regions which were more activated while watching human generated blocks compared to random shapes (blue-green scale). Most significant activated regions are marked on the inflated map; Lateral Occipital cortex (LOC), Inferior frontal gyrus (IFG). (c) LOC ROI analysis: repeated measures ANOVA between averaged beta values of each category; *Human-top rated*, *Human-chosen*, *Human-not chosen*, *Algorithm-random*. Left side - experiment 1 ( $N = 17$ ,  $p < 0.05^*$ ), right side - experiment 2 ( $N = 15$ ,  $p < 0.005^{**}$ ).

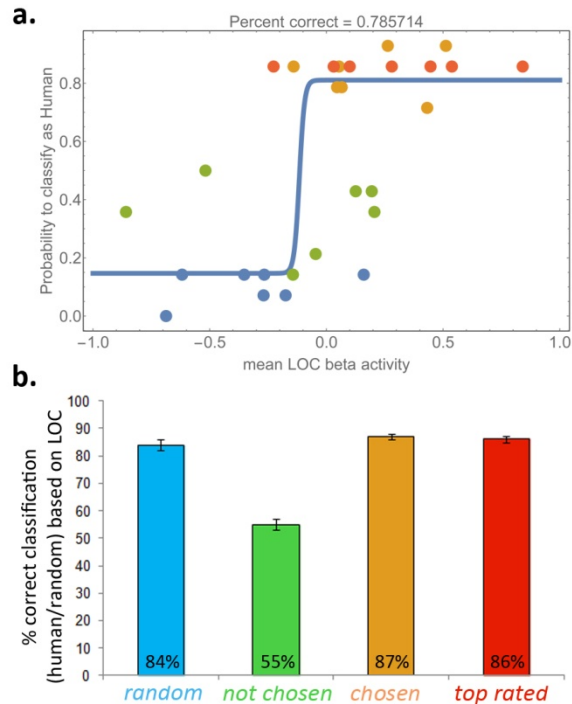


615  
616  
617  
618  
619  
620  
621  
622  
623  
624  
625  
626  
627  
628  
629

**Figure 4. Parametric mapping.** Cortical activity maps of multi subjects, random effect, parametric GLM analysis of beauty (a), weirdness (b), and iconicity (c) presented on an unfolded cortex, right side experiment 1 (N = 13, 13, 14), bottom panel experiment 2 (N = 12, 12, 13), both maps are corrected for multiple comparisons,  $p < 0.05$ . Color scale indicates t values. Yellow- orange scale represents regions which showed positive parametric relation with beauty/weirdness/iconicity scores. Blue-green scale represents regions which showed negative parametric relation with beauty/weirdness/ iconicity scores.

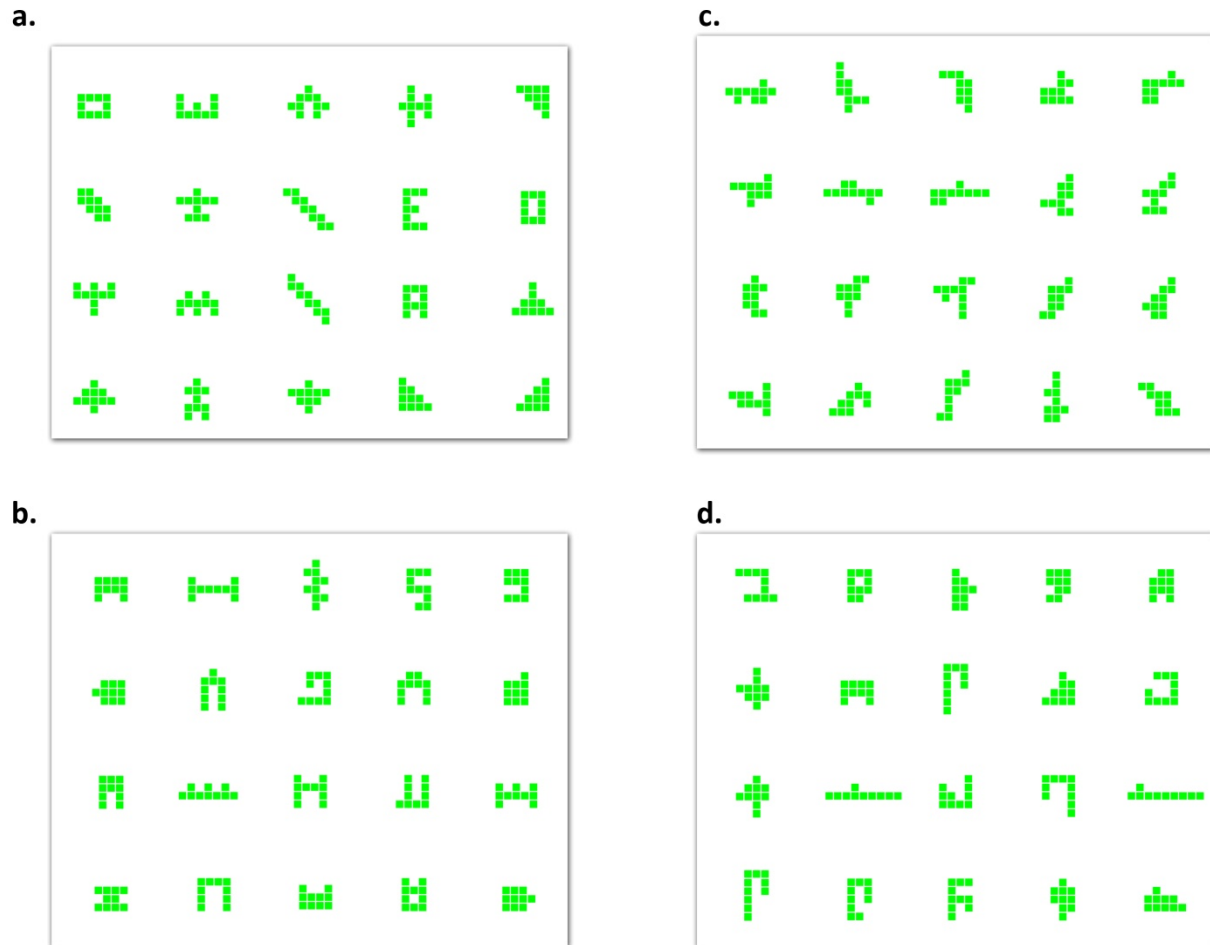


630  
 631 **Figure 5. Correlations of LOC activity and symmetry/beauty.** (a) Scatter plots present the relation between  
 632 averaged blocks' symmetry (x axis) and group's averaged brain activity (normalized beta weight, y axis) in bilateral  
 633 LOC. Each dot represents one block, and color indicates the blocks' category (*Top rated* in red, *chosen* in orange,  
 634 *not chosen* in green, *random* in blue) N = 13. Spearman correlation; (experiment 1) left LOC,  $r = 0.4$ , ns ; right  
 635 LOC,  $r = 0.5$ ,  $p < 0.05$ . (experiment 2) left LOC,  $r = 0.6$ ,  $p < 0.005$ ; right LOC,  $r = 0.5$ ,  $p < 0.05$ . (b) The relation  
 636 between group's averaged beauty ratings (x axis), and the group's averaged brain activity (normalized beta weight, y  
 637 axis) in LOC. Each dot represents mixed blocks with similar beauty ranking, color indicates the blocks' category. N=  
 638 16. Spearman correlation; (experiment 1) left LOC,  $r = 0.52$ ,  $p < 0.005$  ; right LOC,  $r = 0.69$ ,  $p < 0.0005$ .  
 639 (experiment 2) left LOC,  $r = 0.69$ ,  $p < 0.0005$ ; right LOC,  $r = 0.83$ ,  $p < 0.0005$ .



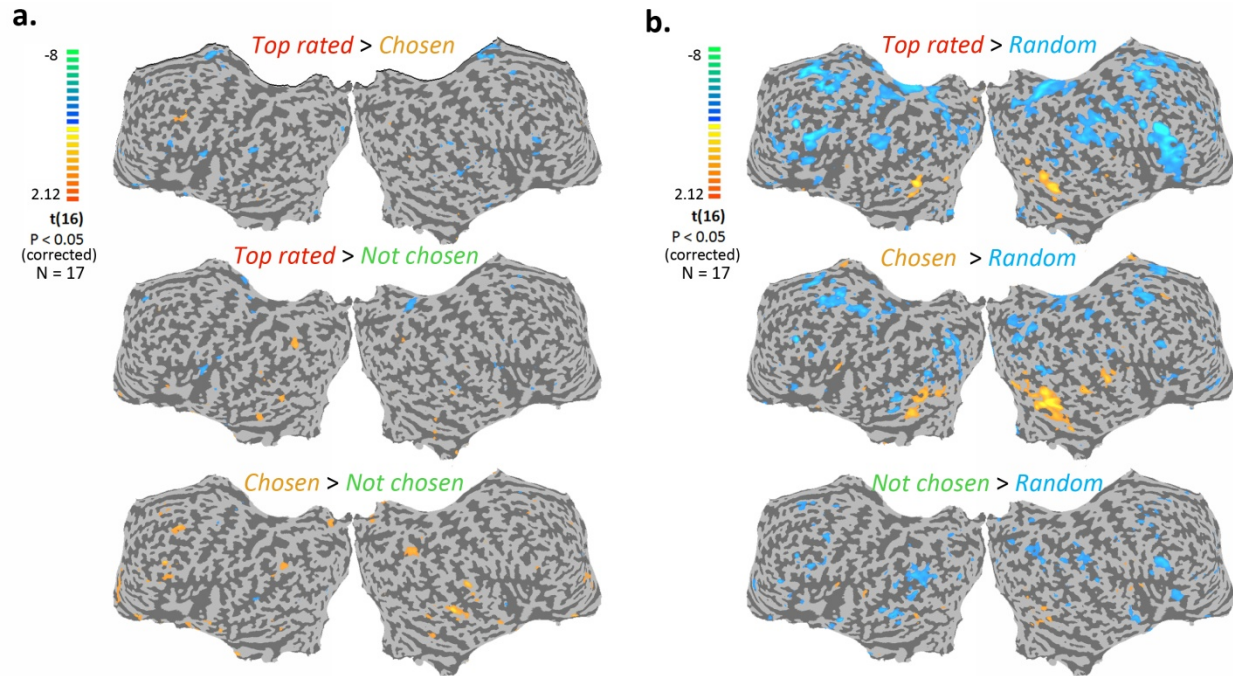
640  
641  
642  
643  
644  
645  
646  
647  
648

**Figure 6. Classification of blocks' origin based on their average LOC activity results in human-level accuracy.** (a) We fitted a hyperbolic tangent classifier,  $P(\text{human}) = a + d \tanh[bx + d]$  (where  $x$  is taken to be the averaged LOC activity of the block) to the data points by a bootstrapping method. Each iteration, 23/28 points were chosen randomly and the best fit parameters were extracted. We repeated this process 1000 times and averaged the parameters of all the runs. Shown is the averaged model. Model parameters are (mean $\pm$ ste):  $a=0.48\pm0.03$ ,  $b=45\pm9$ ,  $c=5\pm1$ ,  $d=0.33\pm0.04$ . (b) Classification accuracy of the classifier on the different categories (top rated, chosen, not-chosen, random). Error bars are STE and are calculated by 100 random sampling with replacements of the real data points per each category.



649  
650  
651

**Supplementary Figure 1. The entire stimuli ensemble.** (a) *Top rated shapes*, (b) *Chosen shapes*, (c) *Random - Never created shapes*, (d) *Not chosen shapes*.



652  
653 **Supplementary Figure 2. Comparison cortical activations between categories (experiment 1).** Multi subjects  
654 activity maps (N = 17, corrected p < 0.05) are presented on an unfolded cortex. Color scale indicates t values. (a)  
655 Contrast maps between all the human generated shapes categories (*Human*). Yellow- orange scale represents regions  
656 which were more activated while watching blocks from the category in the left side of the contrast. Blue-green scale  
657 represents regions which were more activated while watching blocks from the category in the right side of the  
658 contrast. (b) Contrast maps between the *Human* categories and *Random* category (computer generated shapes).  
659 Color scale indicates t values. Yellow- orange scale represents regions which were more activated while watching  
660 shapes of *human* categories, compared to *random* shapes (blue-green scale).  
661  
662  
663  
664  
665  
666  
667  
668  
669  
670  
671  
672  
673  
674  
675  
676  
677  
678  
679  
680  
681

682 **Supplementary Information**

683 Modelling shapes' probability to be classified as human created using the behavioral scores of  
 684 subjects

685 Here we describe the model selection process of finding the best model for the probabilities to be  
 686 classified as human-created vs. random created shapes. The probability function was fit using a  
 687 Logit function,  $P(x, y) = \frac{1}{1+e^{f(x,y)}}$ . The variables of the model were the three subjective scores in  
 688 our experiment – beauty (denoted as  $b$ ), weirdness (denoted as  $w$ ) and iconicity (denoted as  $i$ ).  
 689 Since weirdness and iconicity carry inverse correlations to the behavioral data (iconicity  
 690 increases the probability to be classified as human, while weirdness decreases that same  
 691 probability), we chose to map the weirdness score in the following way -  $w' \rightarrow e^{-w}$ .

692 We tested all possible linear combinations of the individual scores, their pair and triplet  
 693 interactions, yielding:

694 (S1)  $f(b, w', i) = m_0 + m_1 b + m_2 w' + m_3 i + m_{12} b * w' + m_{13} b * i + m_{23} w' * i +$   
 695  $m_{123} b * w' * i$

696 We assessed each model's correlation with the data as well as its Akaike Information Criterion  
 697 (AIC) score to attain the most accurate and simplest best fit model. The most accurate model  
 698 with least number of parameters is one containing the interaction term between beauty and  
 699 weirdness as a sole parameter, suggesting that it is the combination of beauty and familiarity that  
 700 is the dominant component of classifying a shape as having human origin. In Table S1 we list the  
 701 highest correlation and AIC scores of the different models for both beauty and weirdness and  
 702 beauty and iconicity.

703 **Table S1: Pearson correlation, p-values and AIC scores of Logit models with beauty,**  
 704 **weirdness and iconicity scores.**

	Model	Model parameters	Spearman correlation	P-value	AIC scores
1	$f(b, w', i) = b * w'$	$\frac{1}{1 + e^{2.6 - 6.6 b w'}}$	0.96	$4 * 10^{-21}$	5.84
2	$f(b, w', i) = i$	$\frac{1}{1 + e^{1.5 - 7 i}}$	0.94	$5 * 10^{-19}$	6.32
3	$f(b, w', i) = i * w'$	$\frac{1}{1 + e^{1.4 - 7 i w'}}$	0.94	$1 * 10^{-18}$	6.4
4	$f(b, w', i) = b$	$\frac{1}{1 + e^{3.8 - 8 b}}$	0.93	$5 * 10^{-17}$	6.54

5	$f(b, w', i) = b * i$	$\frac{1}{1 + e^{1.3 - 9.2 b i}}$	0.92	$5 * 10^{-16}$	7.04
6	$f(b, w', i) = b * w' * i$	$\frac{1}{1 + e^{1.2 - 9.3 b i w'}}$	0.92	$1 * 10^{-15}$	7.13
7	$f(b, w', i) = w'$	$\frac{1}{1 + e^{7.1 - 9 w'}}$	0.89	$2 * 10^{-12}$	5.36

705

706